ELSEVIER

Physica D 95 (1996) 319–335

PHYSICA D

Periodic travelling waves in a family of deterministic cellular automata

Jonathan A. Sherratt *

Nonlinear Systems Laboratory, Mathematics Institute, University of Warwick, Coventry CV4 7AL, UK

Received 9 May 1995; revised 24 February 1996; accepted 1 March 1996
Communicated by M. Mimura

Abstract

Reaction–diffusion equations whose kinetics contain a stable limit cycle are an established class of models for a range of biological and chemical systems. In this paper I construct a family of deterministic cellular automata, with nine states, which are qualitatively similar to oscillatory reaction–diffusion equations, in that their rules reflect both local oscillations and spatial diffusion. The automata can be crudely interpreted as models of predator–prey interactions, and I show that the behaviour following local perturbation of the prey-only state in one space dimension is very similar in the automata and in standard reaction–diffusion models for predator–prey systems. In particular, in many cases, invasion of prey by predators leaves behind periodic travelling waves in the wake of invasion. I study in detail these periodic plane waves in the automaton, by explicitly investigating periodic solutions of the difference equation governing travelling waves. I show that the automaton has many different periodic wave solutions, and I compare their properties with those of periodic wave solutions of reaction–diffusion systems. The basic conclusion is that included amongst the periodic waves in the automaton are a family of solutions which mimic quite closely the properties of reaction–diffusion periodic waves.

Keywords: Cellular automata; Periodic waves; Reaction–diffusion; Predator–prey; Parabolic partial differential equations

1. Introduction

Cellular automata are now an established class of mathematical models for a wide range of biological, chemical and physical systems. However, the relationship between cellular automata and differential equation models of related phenomena remains unclear. There are two basic approaches to this problem: firstly the development of formal links between particular automata and particular differential equations, and secondly the study of corresponding phenomena in automata and differential equations with qualitative similarities, but without any formal relationship. A number of authors have pursued the first approach by deriving ordinary differential equations for the temporal behaviour of the spatially averaged state of an automaton [1–3]. This has led to important progress on issues such as the route to chaos in cellular automata; however, it of course gives no insight into spatial structure. A slight extension which gives a limited degree of spatial information is the "pair approximation method", in which one follows the temporal evolution of nearest neighbour pairs, again spatially averaged [4,5].

In this paper, I take the second approach, and consider similarities and differences between oscillatory

* E-mail: jas@maths.warwick.ac.uk.

PII S0167-2789(96)00070-X

reaction–diffusion equations and a family of cellular automata, whose rules reflect oscillatory local dynamics and spatial diffusion. Such models are relevant to a range of applications including oscillatory chemical reactions [6,7], intracellular calcium waves [8,9], predator–prey interactions [10,11], and forest regeneration [12,13]. To be specific, I will phrase the discussion in terms of predator–prey dynamics, although the automata I consider deliberately have a very basic form, which could be interpreted in relation to any of the other applications. I will focus in particular on periodic waves in one spatial dimension, which are the fundamental class of solutions for oscillatory reaction–diffusion equations [14,15]. I will show that the cellular automata I consider also have a wide range of periodic travelling wave solutions, and I will compare these with the periodic waves in reaction–diffusion systems.

Previous work comparing solutions in cellular automata and reaction–diffusion equations has focused on planar wavefronts, Turing patterns and waves in excitable media. Propagation of wavefronts has been considered in detail in a recent paper by Schönfisch [16], including an exact derivation of front shape and speed in a deterministic cellular automaton. Wavefronts in automata are dependent on the shape of the spatial grid, and this has been addressed by Markus [17] who has used randomly distributed grid points to eliminate this dependence. Cellular automata reflecting the phenomena of short-range activation and long-range inhibition have been used to simulate spatial patterns [18,19] similar to those resulting from a Turing bifurcation in reaction–diffusion systems [20,21]. Waves in excitable media have been considered in a series of papers by Tyson and colleagues [22–24]. They have developed a cellular automata model for excitable media, whose behaviour is strongly similar to that of reaction–diffusion models. In [24], they discuss periodic plane waves in the automaton, including numerical calculation of dispersion relations; however this is quite different from the work in the present study because excitable and oscillatory systems have fundamentally different characters.

In Section 2 of the paper, I review previous work on oscillatory reaction–diffusion equations, in particular periodic plane wave solutions. In Section 3, I describe the family of automata that I have studied, and discuss numerical simulations of invasion processes which naturally generate periodic waves, in a manner analogous to that in reaction–diffusion systems. In Section 4, I go on to study these periodic wave solutions of the cellular automata, and in Section 5, I comment briefly on the stability of periodic waves in the automata.

2. Periodic waves in reaction-diffusion systems

I use the term "oscillatory" to denote a reaction–diffusion system whose kinetics have a stable limit cycle. Such systems have been studied in great detail, and have a wide range of solution types, including spiral and scroll waves [25,26], spatiotemporal chaos [27–29] and periodic plane waves [14,30]. This paper is concerned with periodic plane waves, which are solutions that move with constant shape and speed, oscillating periodically in space and time. Kopell and Howard [14] showed that such solutions exist for wave speeds greater than a critical value in all oscillatory reaction–diffusion systems, arising via a Hopf bifurcation in the travelling wave ordinary differential equations. For speeds close to the critical, minimum speed, the periodic waves are small amplitude, approximately sinusoidal functions of $t + x/c$, where c is the wave speed, so that both spatial and temporal periods are $\mathcal{O}(1)$ as c approaches its critical value. In contrast, as $c \to \infty$, the waves tend towards the limit cycle of the kinetics, as a function of $t + x/c$; thus the temporal period remains finite, while the spatial period $\to \infty$. It is important to stress that not all of these periodic waves are stable as reaction–diffusion solutions. In particular, waves with speeds sufficiently close to the critical, minimum value are unstable, while waves with sufficiently large speeds are stable; however, a general stability criterion has not been derived, despite considerable effort [31–34].

For the benefit of readers unfamiliar with periodic plane waves, I will illustrate these points by briefly summarising standard results on periodic waves in λ–ω reaction–diffusion systems. This class of equations

has a simple form, enabling periodic wave solutions to be calculated explicitly; as such, they have been used by many authors as a prototype oscillatory reaction–diffusion system [35–37]. Specifically, the equations have the form

$$\partial u/\partial t = \partial^2 u/\partial x^2 + \lambda(r)u - \omega(r)v, \tag{1a}$$

$$\partial v/\partial t = \partial^2 v/\partial x^2 + \omega(r)u + \lambda(r)v, \tag{1b}$$

where $r = (u^2+v^2)^{1/2}$, and $\lambda(\cdot)$ is a decreasing function with a simple zero at r_0. This system has a one-parameter family of periodic plane wave solutions, given by

$$\begin{aligned} u &= R\cos\left[\omega(R)t \pm \lambda(R)^{1/2}x\right], \\ v &= R\sin\left[\omega(R)t \pm \lambda(R)^{1/2}x\right] \end{aligned} \tag{2}$$

with $0 < R < r_0$. As a specific example, consider $\lambda(r) = 1-r^2$, $\omega(r) = 1+r$, in which case the speed of periodic waves is $c = [(1+R)/(1-R)]^{1/2}$, with $0 < R < 1$. Thus the critical minimum speed is $c = 1$, and the spatial and temporal periods are given by $\mathcal{P}_x = \pi(c+1/c)$, $\mathcal{P}_t = \pi(1+1/c^2)$, respectively. The condition for (2) to be stable as a solution of (1) was calculated by Kopell and Howard [14], and in this case reduces to $R^2 > \frac{1}{2}(\sqrt{5}-1)$, or $c > 2.058\ldots$; however, it is important to stress that the stability condition does not always simplify to single inequality on the wave speed c.

Equations of λ–ω type are prototype systems, without specific applications. In contrast, practical oscillatory reaction–diffusion systems often contain at least one steady state outside the limit cycle, in addition to that from which the limit cycle has bifurcated. A typical example is a predator–prey system, in which case the kinetics may have a stable limit cycle, corresponding to coexistence behaviour of predators and prey, but there is also an (unstable) prey-only steady state outside the limit cycle. A standard model of this form is

$$\partial u/\partial t = \partial^2 u/\partial x^2 + u(1-u) - auv/(u+c), \tag{3a}$$

$$\partial v/\partial t = \partial^2 v/\partial x^2 + bv(1-v/u) \tag{3b}$$

(e.g. [38, Ch. 3]). Here $u(x,t)$ and $v(x,t)$ are the population densities of prey and predators respectively; a, b and d are positive parameters, and the kinetics have a stable limit cycle for a range of a–b–d values. A typical phase portrait in such a case is illustrated in Fig. 1(a). For oscillatory predator–prey systems such as (3), I have shown in a series of recent papers that a spatially localised perturbation of the steady state induces a wavefront of invading predators, with periodic plane waves in both prey and predator populations in the wake of the invading front [39–41] (Figs. 1(b) and (c)). The speed of the periodic plane waves is quite different from that of the invading front, and is uniquely selected by a mechanism described in detail elsewhere [39,42,43]. In some cases, the selected speed corresponds to an unstable periodic wave, in which case the solution degenerates into spatiotemporal chaos [29] (Figs. 1(d) and (e)). This phenomenon of oscillatory and chaotic wakes behind invasive fronts applies to a wide range of oscillatory reaction-systems, not just predator–prey models, and appears to be a general mechanism [42]. In the cellular automaton I will describe in Section 3, a very analogous invasion process occurs, that also gives rise to periodic plane waves.

3. A family of oscillatory cellular automata

I now introduce a family of cellular automata whose rules reflect the two basic ingredients of oscillatory reaction–diffusion systems: spatial diffusion and oscillatory local dynamics. The two process are represented as separate, successive steps within a single time iteration, in a manner familiar from coupled map lattice models (e.g. [10,11]), and I will consider a number of different rules for the local oscillations, giving a family of automata. The automata are designed to crudely simulate reaction–diffusion models of predator–prey dynamics, of the type whose kinetics are illustrated in Fig. 1(a), and to be specific I consider the case of three predator and three prey states; this number has no special significance. Therefore the automata have a total of nine states, which are conveniently labelled as $(-1,-1)$, $(-1,0)$, $(-1,1)$, $(0,-1)$, $(0,0)$, $(0,1)$, $(1,-1)$, $(1,0)$, $(1,1)$. Here the first and second components denote the prey and predator states, respectively. The numbers -1, 0 and 1 correspond to successively increasing predator and prey population

densities; note in particular that 0 does not denote an absence of predators or prey.

The first part of each time iteration is a step representing oscillatory local dynamics. In this step, the state at each point in the space lattice changes independently of neighbouring states, according to rules that are illustrated in Fig. 2. Thus I will consider eight different sets of rules, denoted by a code A–H, and for example the rules corresponding to kinetics code B are that state $(0, 0)$ changes to state $(0, 1)$, state $(0, 1)$ changes to $(-1, 0)$, $(-1, 0)$ changes to $(0, -1)$, $(0, -1)$ changes to $(1, 0)$, $(1, 0)$ changes to $(0, 1)$, and states $(1, 1)$, $(1, -1)$, $(-1, 1)$ and $(-1, -1)$ remain unchanged. The key feature of these kinetic rules is their qualitative similarity to the phase portrait illustrated in Fig. 1(a). The state $(1, -1)$ is an

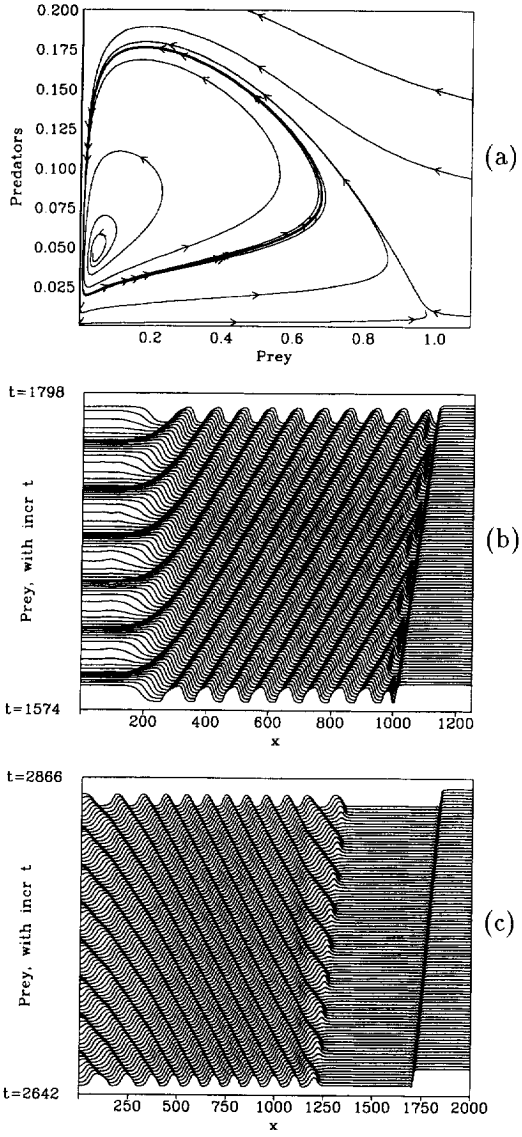

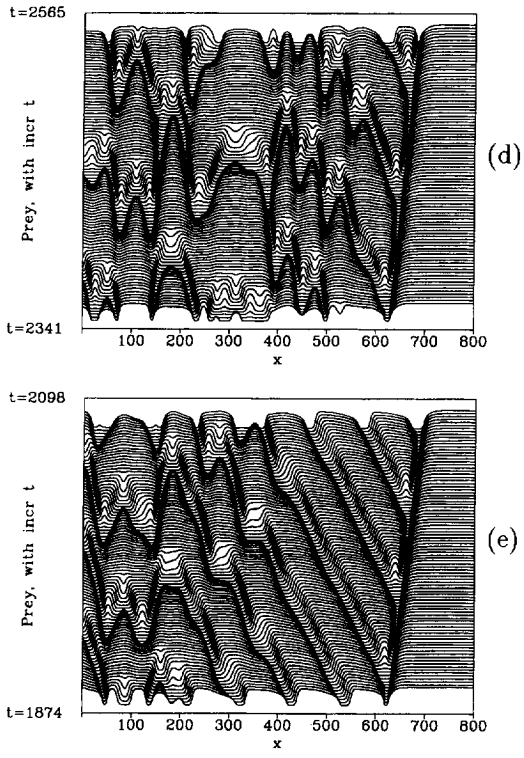

Fig. 1. An illustration of oscillatory waves behind invasion in reaction–diffusion models of predator–prey interactions. The solutions I plot are for the system (3) for various parameters sets for which the local dynamics are oscillatory. A typical phase portrait for the kinetics is illustrated in (a); there is stable coexistence limit cycle, enclosing the unstable coexistence steady state, and another "prey-only" steady state, also unstable. Parts (b) and (c) illustrate cases in which there are periodic travelling waves behind the invasive front, moving in the same and opposite directions as the front, respectively. Part (d) illustrates a case in which there are irregular spatiotemporal oscillations behind the front; in fact the behaviour is temporally chaotic [29,41]. Part (e) shows a mixed case, in which there are periodic waves immediately behind invasion, with irregular spatiotemporal oscillations further back. The parameter values are: (a) $a = 3$, $b = 0.2$, $c = 0.1$; (b) $a = 3$, $b = 0.1$, $c = 0.1$; (c) $a = 3$, $b = 0.1$, $c = 0.2$; (d) $a = 3$, $b = 0.02$, $c = 0.1$; (e) $a = 3$, $b = 0.03$, $c = 0.1$. The equations were solved numerically using the method of lines and Gear's method. The behaviour illustrated here is discussed in much greater detail elsewhere [41].

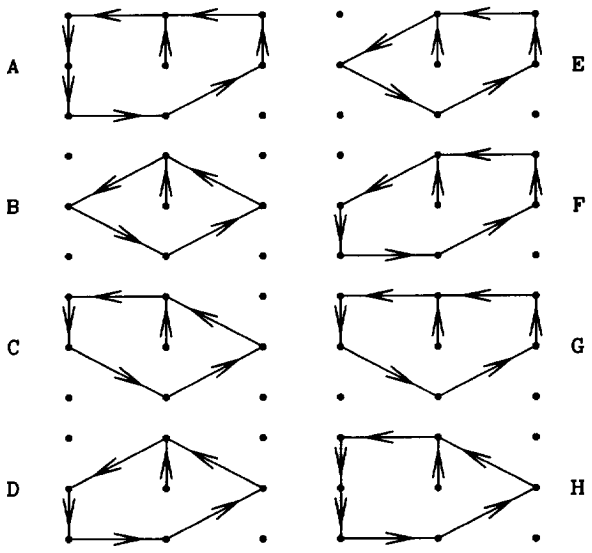

Fig. 2. An illustration of the kinetic rules for my family of cellular automata. The nine grid points represent the nine automaton states, labelled in "predator–prey coordinates" as explained in the text, with the prey state -1, 0, 1 running across the page, and the predator state -1, 0, 1 running up the page. There are eight different sets of kinetic rules, labelled by the letters A–H, which I will refer to as the kinetics codes. During the local dynamics portion of the time iteration, the state changes by moving one step in the direction of the arrow; if there is no arrow leaving a state then it remains unchanged during this portion of the iteration.

equilibrium state for each set of rules, and corresponds to a prey-only steady state. However, otherwise I interpret "-1" as a low but non-zero density; thus the automaton does not have a state corresponding to the absence of both populations. The state (0, 0) is roughly analogous to the unstable coexistence equilibrium in the reaction–diffusion system, although in the automaton it is not a steady state.

Despite these points of similarity, the discrete kinetic rules are of course a simplification of the phase portrait in a number of ways. For example, the predator–prey oscillation moves round its discrete cycle at a uniform speed, whereas in practice predator–prey dynamics are slower at low population densities. Moreover, the particular forms of the various rules A–H are chosen arbitrarily, and some are more ecologically defensible than others. For instance, a state with high predator and low prey density is unlikely to be an equilibrium, which argues against rules B, D, E and F. I consider the full range of kinetic rules in order to give maximum information about the non-linear dynamics similarities and differences between cellular automata of this type and oscillatory reaction–diffusion equations, focusing in particular on periodic waves.

The second part of the time iteration is a discrete representation of spatial diffusion, and in this the prey and predator populations change independently. I consider only dynamics in one space dimension, with an infinite linear sequence of spatial patches, and I denote by h_i and p_i the prey and predator states in patch i, prior to the diffusion step. Thus h_i and p_i have possible values -1, 0 and 1. My representation of diffusion is then

$$h_i^{\text{new}} = (1-\mu)h_i + \tfrac{1}{2}\mu(h_{i+1} + h_{i-1}),$$
$$p_i^{\text{new}} = (1-\mu)p_i + \tfrac{1}{2}\mu(p_{i+1} + p_{i-1}),$$

which is taken directly from standard coupled map lattice models (e.g. [10,11]). The parameter $\mu \in (0, 1]$ is a motility coefficient; for simplicity I assume that this is the same for predators and prey, although this assumption could easily be relaxed. The quantities h_i^{new} and p_i^{new} are initially calculated as real numbers, and then truncated to integers, with $[-1, -0.5)$ truncated to -1, $[-0.5, 0.5]$ truncated to 0, and $(0.5, 1]$ truncated to 1. This truncation means that there is no continuous dependence on μ: specifically, there is no variation as μ changes between critical values given by

$$\pm\tfrac{1}{2} = (1-\mu)I + \tfrac{1}{2}\mu J,$$

where I has any of the values -1, 0 or 1, and J has any of the values $-2, -1, 0, 1, 2$. This gives the critical values as $\frac{1}{4}$, $\frac{1}{3}$, $\frac{1}{2}$, $\frac{3}{4}$, and 1; all that is significant is which of these μ lies between.

Finally, in the interests of brevity it will be helpful when studying travelling waves to represent the nine automaton states by single digits, and the notation I use for this, which is quite arbitrary, is shown in Fig. 3. The numerical values here have no significance; I am just using the digits 1–9 as symbols.

I have not attempted a detailed study of the evolution of this family of automata from a range of different

(−1,1)≡4 (0,1)≡3 (1,1)≡9

(−1,0)≡5 (0,0)≡2 (1,0)≡8

(−1,−1)≡6 (0,−1)≡7 (1,−1)≡1

Fig. 3. An illustration of the single digit representation I use for the automaton states. The numerical values are quite arbitrary: the digits are used purely as symbols. I use this single digit representation in the interests of brevity.

initial conditions. Rather, I have focused on a single initial condition, which mimics the local introduction of predators into an otherwise uniform distribution of prey. Solutions of a reaction–diffusion predator–prey model with such initial conditions are illustrated in Fig. 1. Specifically I have considered setting each spatial patch in the automata to be in state $(1, -1)$, except for the three patches in the centre of the spatial domain, which are set to $(0, 0)$. Recall that $(1, -1)$ is an equilibrium state, corresponding to prey and no predators, while $(0, 0)$ corresponds to a predator–prey mix. The use of $(0, 0)$ as the perturbing state is arbitrary, and different perturbing states do induce different behaviour, although all of the observed behaviour types are given by $(0, 0)$. I consider an infinite one-dimensional sequence of spatial patches; in simulations, the use of a finite patch number simply limits the maximum number of time iterations, since the perturbation cannot spread at a rate greater than one patch per iteration. The end patches are thus maintained at state $(-1, 1)$ in the simulations.

For $\mu < \frac{1}{2}$, it is easy to see that any localised perturbation of the prey-only state $(-1, 1)$ will remain localised, and not spread into neighbouring patches. Therefore it is only necessary to consider the cases $\mu \in [\frac{1}{2}, \frac{3}{4})$, $\mu \in [\frac{3}{4}, 1)$ and $\mu = 1$. For each set of kinetic rules, the first two cases give only minor differences of detail near the site of perturbation, and the results for the first case are illustrated in Fig. 4. In each case the initial perturbation moves outwards, invading the domain at a rate of one patch per time iteration. Behind the invading front, the solution has the form of periodic travelling waves, for some kinetics moving in the direction of invasion, and for

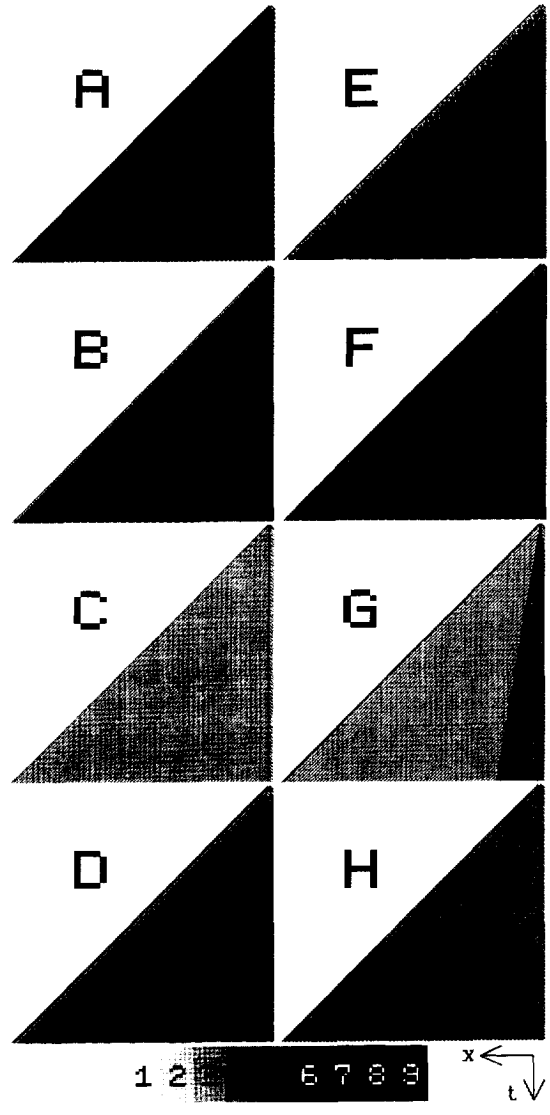

Fig. 4. Invasion of prey by predators in the cellular automaton model, with $\mu \in [\frac{1}{2}, \frac{3}{4})$, for each of the kinetics codes A–H. I show a space–time plot of the automaton state 1–9, which is represented using grey-scale colouring, as indicated in the key. The spatial domain is 801 patches wide, although only patches 1–409 are shown in the figure, running from left to right across the page; 397 time iterations are plotted. Initially every patch is in state 1 (the "prey-only" state) except patches 400–402, which are in state 2. The symmetry of these initial conditions means that the solution is symmetric at all subsequent times. In each case, the initial perturbation induces an invading wavefront, with periodic travelling waves behind this; for kinetics G, there are spatially homogeneous oscillations further back. The details of the periodic waves are given in Table 1(a).

Table 1
Detailed forms of the periodic travelling waves generated behind invasion in the cellular automaton

Kinetics	Behaviour vs x	x period	Behaviour vs t	t period
(a) $\mu \in [\frac{1}{2}, \frac{3}{4})$				
A	3456789	7	3456789	7
B	888777555333	12	3578	4
C	22345	5	22345	5
D	$8^2 7^6 6^2 5^6 3^2 8^6 7^2\ 6^6 5^2 3^6$	40	35678	5
E	$9^6 8^2 7^6 5^2 3^6 9^2 8^6 7^2 5^6 3^2$	40	35789	5
F	998877665533	12	356789	6
G	22345	5	22345	5
H	234567	6	234567	6
(b) $\mu = 1$				
A	223355	6	223355	6
C	545343433232322722257524	24	773355224422332233552244	24
G	545343433232322722257524	24	773355224422332233552244	24
H	223355	6	223355	6

Note: The solutions are illustrated in Figs. 4 and 5. For kinetics codes B, D, E and F with $\mu = 1$, the behaviour behind invasion does not have the form of a periodic wave, and is discussed in detail in the text. In the table I am using the single digit representation of the automaton state, as explained in Fig. 3, and the notation s^n, denoting state s repeated n times.

others moving in the opposite direction. For kinetics G, there is also an expanding region of spatially homogeneous oscillations further back. These solutions are very strongly reminiscent of the generation of periodic waves in the wake of invasion in reaction–diffusion models, as illustrated in Figs. 1(b) and (c). Detailed examination of the data files confirms that in each case the solution is a periodic function of space and time, that is a periodic travelling wave; the detailed forms are listed explicitly in Table 1(a). Note that the integer nature of the calculation means that in contrast to numerical solution of differential equations, the results of these automata simulations are exact, so that the periodic waves given in Table 1(a) are exact solutions. In this table I introduce a notation that I will use frequently, namely s^n, denoting the state s repeated n times. Thus $9^3 56^2$ denotes the sequence 999566 of states, using the single digit representation of states, which is explained in Fig. 3.

For $\mu = 1$, there is a richer range of behaviour, as illustrated in Fig. 5. Again the perturbation invades the domain at a rate of one patch per iteration, and for kinetics codes A, C, G and H there are periodic travelling waves behind the invasion, whose forms are detailed in Table 1(b). For kinetics code B, there is a steady spatiotemporal pattern behind the invasion front, with each patch oscillating between two of the states 3, 5, 7 and 8; these are the states involved in the kinetic oscillations. At even numbered patches the temporal sequence is 55885588..., and at odd numbered patches it is 33773377... This type of solution has no direct analogue in reaction–diffusion solutions. For kinetics codes E and F, the behaviour behind the invading front is irregular and apparently chaotic; this phenomenon certainly occurs in reaction–diffusion solutions, as illustrated in Fig. 1(d). Finally, for kinetics code D, there are small scale oscillations immediately behind the invading front, with a very large scale periodic wave behind these; this periodic wave has a very long spatial and temporal period, and has not exactly repeated itself within the time period illustrated in Fig. 5. There are also some more irregular oscillations in the centre of the domain, around the initial perturbation site, and solution over longer times (which requires a greater number of patches) shows that the region occupied by these grows very slowly. This solution is somewhat reminiscent of reaction–diffusion solutions in which a band of regular oscillations is followed by irregular behaviour, as illustrated in Fig. 1(e).

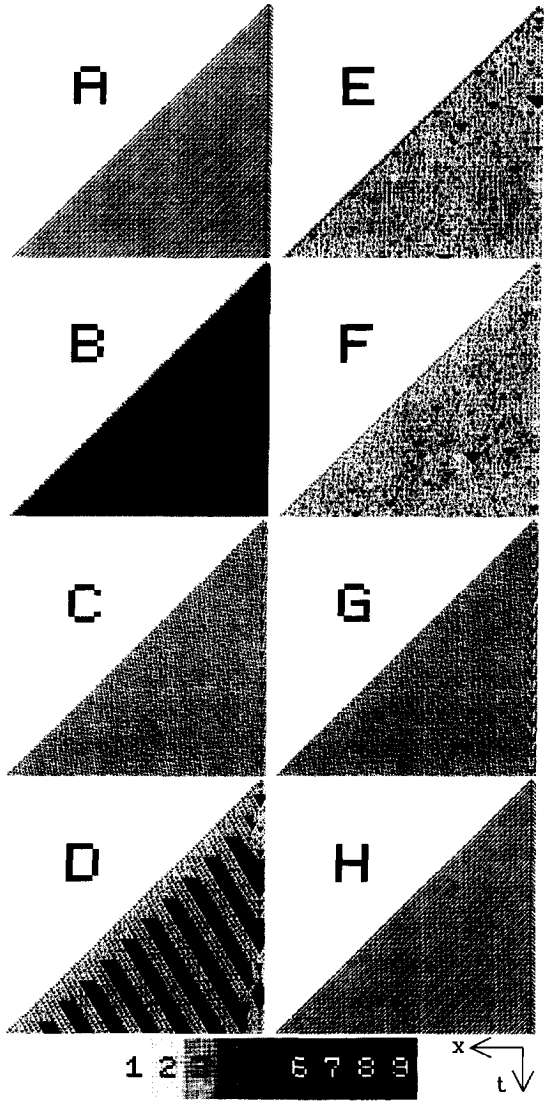

Fig. 5. Invasion of prey by predators in the cellular automaton model, with $\mu = 1$, for each of the kinetics codes A–H. As in Fig. 4, I show a space–time plot of the automaton state 1–9, which is represented using grey-scale colouring, as indicated in the key. The spatial domain is 801 patches wide, although only patches 1–409 are shown in the figure, running from left to right across the page; 397 time iterations are plotted. Initially every patch is in state 1 (the "prey-only" state) except patches 400–402, which are in state 2. The symmetry of these initial conditions means that the solution is symmetric at all subsequent times. In each case, the initial perturbation induces an invading wavefront, with a wide range of different behaviours behind this, which are discussed fully in the main text. For kinetics A, C, G and H, there are periodic travelling waves behind the invading front, and the details of these periodic waves are given in Table 1(b).

4. Analysis of periodic travelling waves

The simulations described above show that in the cellular automaton, periodic waves arise naturally in the wake of invasive fronts, in a manner directly analogous to that in corresponding reaction–diffusion models. In this section I will describe a method for analysing periodic travelling wave solutions of the automata I am studying. The object is to determine the range of wave solutions that exist, and to investigate some of their properties; throughout, I will be comparing with the properties of periodic wave solutions of reaction–diffusion systems, which are reviewed in Section 2. To my knowledge, this is the first study of periodic waves in oscillatory cellular automata.

In a cellular automaton, a periodic travelling wave is a solution in which the automaton state s_x^t is a function $S(\alpha x \pm \beta t)$. Here x and t are integers denoting the patch number and iteration number, respectively, and α and β are positive integers; for uniqueness, I restrict α and β to be coprime. The sign ("$\pm$") determines the direction of motion of the wave. The automata I am considering can be written in the general form

$$s_x^{t+1} = F(s_x^t, s_{x-1}^t, s_{x+1}^t; \mu)\,.$$

The function F depends on the kinetics code as well as the parameter μ; note in particular that the dependence on s_x^t disappears in the special case $\mu = 1$, which will have important implications for periodic waves. Although the function F cannot be expressed in a simple formula, it can easily be calculated using the automaton rules described above. Solutions of the form $s_x^t = S(\alpha x \pm \beta t)$ therefore satisfy

$$S(z+\beta) = F(S(z), S(z-\alpha), S(z+\alpha))\,. \qquad (4)$$

Here the "$\pm$" plays no role because F depends symmetrically on s_{x+1}^t and s_{x-1}^t; this corresponds to the symmetry of positive and negative spatial directions. The integer variable z is a travelling wave coordinate, and the difference equation (4) is the travelling wave equation, analogous to the travelling wave ordinary differential equation for reaction–diffusion systems. Periodic travelling waves of the cellular automaton therefore correspond to periodic solutions of (4), in the same way that periodic waves in reaction–diffusion

systems correspond to limit cycle solutions of the travelling wave ODES.

Therefore, my aim in this section is to investigate periodic solutions of (4). My investigation is purely numerical; however, the integer nature of the arithmetic means that the numerical results are exact. I will consider only the two cases $\mu \in [\frac{1}{2}, \frac{3}{4})$ and $\mu = 1$, which are exactly the cases illustrated in Figs. 4 and 5. I must stress at the outset that I have been unable to determine all periodic solutions of (4), and my results are more in the nature of experimentation, giving a flavour of the periodic solutions and their properties. The numerical approach is rather different in the cases $\alpha < \beta$ and $\alpha \geq \beta$, and I will describe these cases separately.

4.1. Periodic waves with $\alpha < \beta$

When $\alpha < \beta$, (4) is a straightforward difference equation, of order $\alpha + \beta$:

$$S(z) = F(S(z-\beta), S(z-\alpha-\beta), S(z+\alpha-\beta)). \tag{5}$$

Since $S(\cdot)$ has a finite set of possible values, there are no standard methods available for investigating periodic solutions of (5). However, the solution is uniquely determined by a sequence of initial values for $S(1), S(2), \ldots, S(\alpha+\beta)$, and is easily calculated from such an initial sequence. Therefore I have approached the problem of investigating periodic solutions of (5) by explicitly solving the difference equation for a range of initial sequences, given a pair of values α, β. The solution evolves to a periodic solution if any consecutive sequence of $\alpha+\beta$ states is repeated; therefore after calculation of each new state $S(z)$, my program loops back through all previous states $z_1 = z-1,\ z-2, \ldots,\ \alpha+\beta$, and compares the sequences $S(z),\ S(z-1), \ldots,\ S(z-\alpha-\beta+1)$ and $S(z_1),\ S(z_1-1), \ldots,\ S(z_1-\alpha-\beta+1)$. If these are the same, then the solution has evolved to a periodic solution with period $z - z_1$, and further calculation is unnecessary because this periodic sequence will simply be repeated in subsequent solution.

I have calculated solutions of (5) in this way for many values of α and β, both values of μ, and many initial sequences; in every case I have found that the solution evolves to a periodic solution. Of course, some initial conditions evolve to constant solutions ("period 1 solutions"); these trivial "waves" will occur precisely for the states left unchanged by the kinetics, and I will exclude them from subsequent discussion. In most cases, there are a number of different periodic waves for given values of α, β and μ, and this number tends to increase with $\alpha+\beta$, as does the period of the waves. For small values of α and β, it is possible to loop through all possible initial sequences (a total of $9^{\alpha+\beta}$), and thereby determine all of the periodic waves for that α and β. However, for larger $\alpha+\beta$, the number of possible initial conditions makes this computationally unfeasible, and I have simply considered a selection of initial sequences, given by a random number generator. In Table 2, I list all the periodic solutions that exist for $\alpha = 1$ and $\beta = 2, 3$, for both values of μ (period 1 solutions are omitted). A number of these solutions were observed as periodic travelling waves behind invasion (listed in Table 1); note that since $\alpha = 1$, the spatial sequence is the same as that of the function $S(\cdot)$. For clarity, let me emphasise that (as an example) for $\alpha = 1$, $\beta = 3$, $\mu \in [\frac{1}{2}, \frac{3}{4})$ and with kinetics code E, all 6561 ($= 9^4$) possible initial sequences ultimately evolve to either the period 15 solution 999333555777888, or to one of the constant solutions 1, 4 and 6. Here I am using the single digit representation of the automaton state, which is explained in Fig. 3.

When β is large with $\alpha = 1$, there are many periodic solutions: for example, when $\beta = 10$, $\alpha = 1$ with $\mu \in [\frac{1}{2}, \frac{3}{4})$, there are at least 15 periodic solutions for each kinetics, and for kinetics code A there are at least 42 periodic solutions, with periods ranging from 70 to 366. I use the phrase "at least" because I am only considering a small fraction of the possible initial sequences. For $\mu = 1$ with $\beta = 10, \alpha = 1$, the number of waves I have found varies more with kinetics: I have only found three periodic solutions for kinetic codes D (periods 47, 51 and 379) and E (periods 40, 80 and 147), while for kinetics code H there are at least 50 periodic solutions, all of period 60. It is important to stress that this does not indicate that in this case there are more periodic solutions for code H than codes D

Table 2
A list of all periodic solutions of the travelling wave equation (3), for $\alpha = 1$, $\beta = 2$, 3, and for both values of μ that I am considering (constant solutions (period 1) are omitted)

Kinetics	Period	Wave form
(a) $\mu \in [\frac{1}{2}, \frac{3}{4})$, $\alpha = 1$, $\beta = 2$		
A	14	99334455667788
B	8	88335577
C	10	8833445577
D	10	8833556677
E	10	9933557788
F	12	993355667788
G	12	993344557788
H	12	883344556677
(b) $\mu \in [\frac{1}{2}, \frac{3}{4})$, $\alpha = 1$, $\beta = 3$		
A	2	52
	21	999333444555666777888
B	12	888333555777
C	15	888333444555777
D	2	52
	15	888333555666777
E	15	999333555777888
F	2	52
	18	999333555666777888
G	18	999333444555777888
H	2	52
	18	888333444555666777
(c) $\mu = 1$, $\alpha = 1$, $\beta = 2$		
A	3	523
	12	722233345556
B	7	5222323
C	8	52223334
	8	52323423
D	7	5222323
E	7	5222323
F	7	5222323
G	8	52223334
	8	52323423
H	3	523
	12	722233345556

and E, since I am only considering a very small set of the possible initial sequences (which number more than 31 billion), and I give these figures simply to give an indication of the range of behaviour that I have found.

How do these results compare with the properties of periodic wave solutions of reaction–diffusion systems? The most striking difference is the existence of many different periodic waves for a given speed ($= \beta/\alpha$) in the cellular automata. Although this is certainly possible in reaction–diffusion systems, in most cases relevant to applications, there is exactly one periodic wave for each speed greater than the critical minimum value; this is certainly true for the predator–prey systems I have worked with, including the system used in Fig. 1. However, as in reaction–diffusion equations, the spatial period of the automaton waves seems to increase with β/α, while the temporal period remains approximately constant. Results suggesting this for $\alpha = 1$ and increasing β are described above,

Table 2
Continued

Kinetics	Period	Wave form	Period	Wave form
(d) $\mu = 1, \alpha = 1, \beta = 3$				
A	18	712121313141515161	18	772222333344555566
	18	762722323343545565	18	752627323243535465
	18	752526373242535364	9	742525363
B	6	312121	6	332222
	3	322	2	41
	6	434242	2	61
	6	636262	2	91
	6	939292	2	64
	2	94	2	96
C	12	512121313141	12	552222333344
	12	542522323343	12	532425323243
	2	61	12	656262636364
	2	91	12	959292939394
	2	96		
D	6	312121	6	332222
	3	322	2	41
	6	434242	2	91
	6	939292	2	94
E	6	312121	6	332222
	3	322	2	41
	6	434242	2	61
	6	636262	2	64
F	6	312121	6	332222
	3	322	2	41
	6	434242		
G	12	512121313141	12	552222333344
	12	542522323343	12	532425323243
	2	61	12	656262636364
H	18	712121313141515161	18	772222333344555566
	18	762722323343545565	18	752627323243535465
	18	752526373242535364	9	742525363
	2	91	18	979292939394959596

and it is also shown by the (smaller number of) simulations that I have done for other values of α; note that the spatial and temporal periods of the wave are given by $\mathcal{P}_s/\alpha$ and $\mathcal{P}_s/\beta$, where $\mathcal{P}_s$ is the period of the travelling wave function $S(\cdot)$.

A powerful general theorem on periodic travelling waves in reaction–diffusion equations is that as the speed of the waves $\to \infty$, the temporal behaviour of the waves approaches the limit cycle solution of the kinetics. Although I cannot make general statements about this for the cellular automaton, it is certainly true that when $\alpha = 1$, there is a family of solutions which approach the kinetic oscillations as $\beta \to \infty$, specifically the solutions given in Table 3. For $\mu \in [\frac{1}{2}, \frac{3}{4})$, the temporal behaviour of the solutions listed in Table 3(a) is exactly the kinetic oscillations, even for small β, but this is not the case for $\mu = 1$ and the solutions listed in Table 3(b). For these solutions, straightforward checking using the automaton rules shows that as β increases, so that the period $\mathcal{P}_s$ increases, there are a constant number of elements $z \in \{1, \ldots, \mathcal{P}_s\}$ for which $S(z+\beta) \neq f_{\text{kinetics}}(S(z))$, where $f_{\text{kinetics}}(S(z))$ denotes the kinetics function defined in Fig. 2. Now in the periodic wave solution, $S(z+\beta)$ is the state following $S(z)$ at the next time iteration in a given spatial patch, and thus the temporal behaviour of the periodic wave approaches the kinetic oscillations as $\beta \to \infty$. Note that, as indicated in Table 3(b), I have been unable to construct a solution with this property for kinetics codes E, F and G, although one may exist.

Table 3
Periodic wave solutions of the travelling wave equation (3) for β large with $\alpha = 1$

Kinetics	Period	Wave form
(a) $\mu \in [\frac{1}{2}, \frac{3}{4})$		
A	7β	$9^\beta 3^\beta 4^\beta 5^\beta 6^\beta 7^\beta 8^\beta$
B	4β	$8^\beta 3^\beta 5^\beta 7^\beta$
C	5β	$8^\beta 3^\beta 4^\beta 5^\beta 7^\beta$
D	5β	$8^\beta 3^\beta 5^\beta 6^\beta 7^\beta$
E	5β	$9^\beta 3^\beta 5^\beta 7^\beta 8^\beta$
F	6β	$9^\beta 3^\beta 5^\beta 6^\beta 7^\beta 8^\beta$
G	6β	$9^\beta 3^\beta 4^\beta 5^\beta 7^\beta 8^\beta$
H	6β	$8^\beta 3^\beta 4^\beta 5^\beta 6^\beta 7^\beta$
(b) $\mu = 1$		
A	$7\beta-3$	$9^{\beta-5}\ 3^{\beta+1}\ 4^{\beta-1}\ 5^{\beta+1}\ 6^{\beta-1}\ 7^{\beta-1}\ 2^2\ 8^{\beta-3}\ 2^2\ 3^2$
B	$4\beta+2$	$8^{\beta-7}\ 2^6\ 3^{\beta-1}\ 2^2\ 5^{\beta-3}\ 2^4\ 7^{\beta-5}\ 2^2\ 3^2\ 2^2$
C	$5\beta-1$	$8^{\beta-5}\ 2^2\ 3^{\beta+1}\ 4^{\beta-1}\ 5^{\beta-1}\ 2^2\ 7^{\beta-3}\ 2^4$
D	$5\beta-3$	$8^{\beta-9}\ 2^2\ 3^{\beta-1}\ 2^2\ 5^{\beta-3}\ 2^4\ 6^{\beta-5}\ 2^2\ 3^2\ 2^2\ 7^{\beta-7}\ 2^8$
H	6β	$8^{\beta-3}\ 2^2\ 3^{\beta+1}\ 4^{\beta-1}\ 5^{\beta+1}\ 6^{\beta-1}\ 7^{\beta-1}\ 2^2$

Note: There are many other periodic solutions of (3) for large β, but these solutions have the property that as $\beta \to \infty$, the temporal behaviour approaches that of the kinetics. I have not been able to construct a solution with this property for $\mu = 1$ and kinetics codes E, F and G. In (a) the waves are exactly the kinetic oscillations (see Fig. 2), with each state repeated β times.

4.2. *Periodic waves with $\alpha = \beta = 1$*

When $\alpha = \beta = 1$, the travelling wave equation becomes

$$S(z) = F(S(z), S(z-1), S(z-2)). \tag{6}$$

This is an implicit equation for $S(z)$ as a function of two previous states. Moreover, the equation has a very different character in the two cases $\mu \in [\frac{1}{2}, \frac{3}{4})$ and $\mu = 1$, since the dependence of F on $S(z-1)$ disappears in the latter case.

I begin by considering this latter case, $\mu = 1$, so that we have

$$S(z) = F(S(z), S(z-2)). \tag{7}$$

Thus, odd and even values of z decouple. Solutions of (7) can easily be studied by determining, for each possible state $S(z-2)$, which of the nine possible states $S(z)$ will satisfy (7): note that in general there will be more than one state $S(z)$ satisfying the equation for given $S(z-2)$. This calculation shows that there are no non-constant periodic solutions of (7) for kinetics B–G, and exactly one for kinetics A and H, namely the period 3 solution 523. There are thus three different periodic travelling waves of speed 1 in these cases, all of period 6, corresponding to different interweavings of the sequence 523 for the odd and even z values: 552233, 532532 and 522335. It is the first of these waves that is generated behind the invasive front in the solutions illustrated in Fig. 5 for these kinetics codes.

A peculiarity of the cellular automaton is that waves with very similar speeds are solutions of quite different equations, because of the requirement that α and β are integers. As an example of this, I consider kinetics code A with $\mu = 1$ and $\alpha = \beta - 1$, with β large. Intuitively, one expects that in this case, periodic waves will have approximately the same form as one of the period 6 waves of speed 1 described above. In fact, for $\alpha = \beta - 1$ with β large, there are a great many different periodic solutions of (5), and many of these do not resemble the speed 1 waves. However I have been able to construct a solution which does approach a speed 1 wave as β (and α) $\to \infty$, namely

$$7\ 2^{\alpha+\beta} 3^{\alpha+\beta} 4\ 5^{\alpha+\beta} 6, \tag{8}$$

which has period 6β. The spatial sequence at a given time iteration is $S(t)$, $S(t+\alpha)$, $S(t+2\alpha)$, ..., which differs from the sequence 552233552233... at only a

Table 4
An illustration of the method used to find periodic solutions of the travelling wave equation (5) for $\alpha = \beta = 1$ when $\mu \in [\frac{1}{2}, \frac{3}{4})$

1	2	3	4	5	6	7	8	9	10	11
72	723	7234	72345	723452	7234522	72345223	723452234	7234522345	72345223452	723452234522
									72345223456	723452234562
										723452234566
										723452234567
				723456	7234562	72345622	723456223	7234562234	72345622345	723456223452
										723456223456
					7234566	72345666	723456666	7234566666	72345666666	723456666666
										723456666667
									72345666667	723456666672
								7234566667	72345666672	723456666723
							723456667	7234566672	72345666723	723456667234
						72345667	723456672	7234566723	72345667234	723456672345
					7234567	72345672	723456723	7234567234	72345672345	723456723452
										723456723456

Note: The table shows the possible solutions for the first 11 iterations, starting from the initial sequence 72, for kinetics G. A blank entry in the table indicates that the entry is the same as that in the previous row. Sequences that are part of periodic solutions are underlined; I include in my underlining the period 1 solution 6. This table shows clearly that a single initial sequence can require many solution sequences to be followed simultaneously.

small number of patches, with this number remaining constant as β and α increase. For the temporal sequence at a given patch, $S(x)$, $S(x+\beta)$, $S(x+2\beta), \ldots$, the situation is slightly different because the period $\mathcal{P}_S$ of $S(\cdot)$ is divisible by β. Thus the temporal sequence has period 6 at every patch, and is exactly 552233552233... at most patches, the exceptions being those patches whose x value causes the states 7, 4 or 6 to appear in their sequence. In fact 4 and 6 appear together if at all, and thus the temporal sequence is 552233552233... at a proportion of the patches given by $(6\beta - 2)/6\beta, \rightarrow 1$ as $\beta \rightarrow \infty$. Therefore (8) does indeed approach the speed 1 wave 552233 as $\alpha = \beta - 1 \rightarrow \infty$. The solution (8) is in fact also a solution for kinetics code H.

I turn now to waves with $\alpha = \beta = 1$ for $\mu \in [\frac{1}{2}, \frac{3}{4})$. In this case, the travelling wave equation (6) is a second order implicit difference equation. It turns out that for a high proportion of the 81 possible pairs of states, $S(z-2)$ and $S(z-1)$, there are several states $S(z)$ satisfying (6), and thus a systematic approach is required to investigate possible periodic waves, rather than the ad hoc method used for $\mu = 1$. The method I use is to start with a given pair of initial values, $S(1)$ and $S(2)$, and test each of the nine states as a possible solution of (6) for $S(3)$. Successful triplets are stored, and the process is repeated for $S(4)$, etc. An example of the iteration process is given in Table 4. For some initial pairs of states, this can eventually lead to the following of many hundreds of possible solutions; at each iteration, some of these disappear from consideration because there is no possible next state, while for others there are several next states possible, thus increasing the number of solutions being followed. Periodic solutions occur when any consecutive pair of states is repeated, although in contrast to the case of $\alpha < \beta$, the solution must be continued when such a repetition is detected, because there may be other possible

subsequent behaviours, including other periodic solutions, in addition to the repeating periodic sequence that has been found.

Application of this method shows that for each set of kinetics there are multiple periodic solutions of (6): for kinetics A, there are at least 400 non-constant periodic solutions, with periods ranging from 5 to 24. This is in very sharp contrast to the behaviour for $\mu = 1$ (three solutions all of period 6) and for reaction–diffusion equations (typically one periodic wave for any given wave speed).

4.3. Periodic waves with $\alpha > \beta$

When $\alpha > \beta$, (4) is again an implicit difference equation, of order 2α:

$$S(z+\beta-\alpha) = F(S(z-\alpha), S(z-2\alpha), S(z)). \quad (9)$$

The implicit nature of this equation makes it considerably more difficult to study than the explicit difference equation (5) governing waves with $\alpha < \beta$. I have used essentially the same approach as that described above for the case $\alpha = \beta$, $\mu \in [\frac{1}{2}, \frac{3}{4})$. That is, starting from a given initial sequence $S(1), S(2), \ldots, S(2\alpha)$, I test all nine states as possible solutions of (9), storing all successful sequences $S(1), S(2), \ldots, S(2\alpha+1)$. For each of these I then proceed with the next iteration. However, this method has unfortunately had only limited success.

There are a total of $9^{2\alpha}$ possible initial states for Eq. (9). Many of these will not generate a long-term solution, due to the solution reaching a point at which there is no state $S(z)$ satisfying (9), so that the solution cannot be continued. However, other initial states will lead to a rapidly expanding number of solutions to be followed, because of multiple states $S(z)$ satisfying (9) at each iteration. The difficulty with the computation is that some initial conditions can give an exponential rise in the number of solutions being followed at successive iterations, getting as high as hundreds of thousands; each of these must be examined at every iteration, making the computations extremely slow for even a single initial sequence.

I have successfully determined all periodic solutions of (9) only for $\beta = 1$, $\alpha = 2$, 3 when $\mu \in [\frac{1}{2}, \frac{3}{4})$, and $\beta = 1$, $\alpha = 2$ when $\mu = 1$; these are listed in Table 5. For clarity, let me emphasise that in these cases, all initial sequences (a total of $6561 = 9^4$ when $\alpha = 2$ and $531441 = 9^6$ when $\alpha = 3$) either fail to generate a long-term solution, or generate one (or more) of the solutions listed in Table 5, and/or a constant solution. The phrases "one or more" and "and/or" in the last sentence are significant: a single initial sequence can generate a number of different long-term solutions (e.g. Table 4).

When α and β are both large, there appear to be many periodic solutions of (9): for example, when $\alpha = 13$ and $\beta = 12$ with $\mu = 1$ and with kinetics code A, I have found more than 40 different periodic solutions, all with period 72. However, in view of the discussion in Section 4.2, I should mention that I have not found a solution which resembles any of the speed 1 waves with $\beta = \alpha - 1$ large, although I conjecture that such a solution does exist.

For large α with $\beta = 1$, I have had very little success at finding periodic solutions of (9). It may be that few such solutions exist; recall that for reaction–diffusion systems there is a minimum speed below which there are no periodic waves. However, this cannot be concluded from my computations, which have considered only an insignificant proportion of the $9^{2\alpha}$ possible initial states. One notable periodic solution that I have detected is the following period 24 solution for $\alpha = 5$, $\beta = 1$, $\mu = 1$ with kinetics codes C and G:

773355224422332233552244,

which is the wave observed behind invasion in these cases (see Fig. 5 and Table 1(b)).

In reaction–diffusion systems, as the wave speed approaches the critical minimum value, periodic waves become low amplitude oscillations about the (unstable) coexistence steady state. In the cellular automaton, there is no corresponding notion of "wave amplitude". However, there is a loose correspondence between the coexistence steady state in the phase portrait of Fig. 1(a) and the automaton state $2 \equiv (0, 0)$ in the kinetic oscillations shown in Fig. 2. Therefore, one might expect that for large α with $\beta = 1$, automaton waves would contain a large proportion of entries in state 2, by analogy with the low amplitude

Table 5
A list of all the periodic solutions of (3) for $\alpha = 2$, $\beta = 1$, $\mu = 1$ (constant solutions (of period 1) are omitted)

Kinetics	Period	Wave form
A	3	532
B	15	753222232322532
	4	8753
	19	87532222323225327 53
C		
D	15	653222232322532
E	15	753222232322532
	19	87532222323225327 53
F	15	653222232322532
G		
H	3	532

Note: For kinetics C and G, there are no non-constant periodic solutions. For $\mu \in [\frac{1}{2}, \frac{3}{4})$, there are no non-constant periodic solutions for $\alpha = 2$, $\beta = 1$, while for $\alpha = 3$, $\beta = 1$, the only non-constant periodic solution is the period 2 solution 52, which is a solution for kinetics codes A, D, F and H.

of low speed reaction–diffusion waves. I have found only a handful of waves with $\beta = 1$ and values of $\alpha > 4$, so that I can do little more than speculate, but the solutions that I have found are consistent with this hypothesis for $\mu = 1$ (e.g. for $\alpha = 7$ with kinetics F, I have found a period 106 solution in which 46 entries are state 2), but not for $\mu \in [\frac{1}{2}, \frac{3}{4})$ (e.g. for $\alpha = 5$ with kinetics B, I have found a period 5 solution in which no entries are state 2).

5. Stability of periodic waves

I now consider briefly the stability of the periodic waves described above, as solutions of the cellular automaton; again, my study is purely numerical. As discussed in Section 2, in reaction–diffusion equations, waves of speed close to the critical minimum value are unstable as PDE solutions, while high speed waves are stable. This of course assumes that the limit cycle solution of the kinetics is stable as a (spatially homogeneous) reaction–diffusion solution; when the equations have equal diffusion coefficients, as in the cases I am considering, this is implied by the stability of the limit cycle as a solution of the kinetic ODES [14].

Therefore the first task is to consider whether the spatially homogeneous oscillations of the kinetics are stable as a solution of the automaton. For a cellular automaton, there is no notion of "small perturbation" or "local stability", since the state space is discrete. Therefore I must define my notion of stability for a solution of the automaton. I consider a perturbation of a single patch to any of the other eight states. In view of the large amplitude nature of this perturbation, it is too restrictive to require the perturbation to decay completely, and I have found that the most useful definition of stability is that the perturbed and unperturbed solutions are identical at all future times, except over a finite sequence of spatial patches whose length remains bounded. Note in particular that this classifies a convecting perturbation as stable; it is quite common that perturbation of a periodic wave alters the state at a small number of patches within one spatial period, and that these then move through space with the wave. My definition of a stable solution is thus that the solution is stable (in the sense just described) to the perturbation of *any* single patch to *any* other state. Thus testing the stability of a periodic wave requires the consideration of $8\mathcal{P}_s$ separate perturbations, since every perturbation of every wave element must be tested.

Under this definition, the kinetic oscillations are stable for each of the kinetics when $\mu \in [\frac{1}{2}, \frac{3}{4})$, while for $\mu = 1$, only the oscillations of kinetics B, D and H are stable. For periodic waves, every wave that I have tested for $\mu \in [\frac{1}{2}, \frac{3}{4})$ and $\alpha \leq \beta$ is stable, with some of the waves for $\alpha \geq \beta$ stable and some unstable. This is broadly consistent with the behaviour in reaction–diffusion equations, for which fast waves

are stable and slow waves are unstable. However, for $\mu = 1$, I have been unable to detect any general trend in the stability of periodic waves.

6. Discussion

In this paper I have compared a family of cellular automata with qualitatively similar reaction–diffusion systems. The similarity lies in the fact that the basic ingredients of both the automata and the PDEs are local oscillations and spatial diffusion. I must stress that there is absolutely no formal relationship between the automata and the PDEs, only this qualitative similarity in formulation.

In view of this lack of formal relationship, there is a remarkable similarity between the response to local perturbation of the "prey-only" state in the two types of model. The most striking aspect of this is the generation of periodic travelling waves. Such waves have been well-studied in reaction–diffusion equations, and I have gone on to do a corresponding study in the cellular automata, by explicitly investigating the difference equation governing travelling wave solutions. My investigation leaves many questions unanswered, but the basic conclusion is that the cellular automata have a great many periodic wave solutions, included amongst which are solutions which mimic quite closely the properties of reaction–diffusion periodic waves. The natural next step in this work would be to consider automata with more predator and prey states, to study the extent to which my results translate to these more complex automata. I have deliberately used reaction–diffusion equations as my point of comparison, because periodic wave behaviour in these equations is well understood. Other common types of predator–prey model are coupled map lattice [10,11] and coupled differential equation models [2,44]; however, periodic wave behaviour is much more poorly understood in these systems, despite some recent progress [45].

The rapid increase in the use of cellular automata and coupled map lattice models in mathematical biology has had a tendency to divide the academic community into those who use discrete models and those who use continuous models. This is clearly an unfortunate and very artificial division, since for many systems, both discrete and continuous models can be justified. The work in this paper shows that in the particular case of oscillatory, diffusing biological systems, the solutions of the two types of model do have many features with very strong qualitative similarities. This in turn provides very strong evidence that it is these features that are genuine consequences of the qualitative ingredients of the models.

Acknowledgements

This work was supported in part by grants from the Nuffield Foundation and the Royal Society of London. I am grateful to David Rand (Warwick), Mark Lewis (Utah), Barry Eagan (Utah) and James Sneyd (Christchurch) for helpful discussions.

References

[1] N. Boccara and K. Cheong, J. Phys. A 26 (1993) 3707.
[2] A.M. De Roos, E. McCauley and W.G. Wilson, Proc. Roy. Soc. London Ser B 246 (1991) 117.
[3] G. Szabo and G. Odor, Phys. Rev. E 49 (1994) 2764.
[4] H. Matsuda, N. Ogita, A. Sasaki and K. Sato, Progr. Theoret. Phys. 88 (1992) 1035.
[5] Y. Harada and Y. Iwasa, Res. Popul. Ecol. 36 (1994) 237.
[6] J.A. Leach, J.H. Merkin and S.K. Scott, J. Math. Chem. 16 (1994) 115.
[7] S. Scott, Chemical Chaos (Clarendon Press, Oxford, 1991).
[8] J. Sneyd, S. Girard and D. Clapham, Bull. Math., Biol. 55 (1993) 315.
[9] J. Sneyd and J.A. Sherratt, SIAM J. Appl. Math. in press.
[10] M.P. Hassell, H.N. Comins and R.M. May, Nature 353 (1991) 255.
[11] H.N. Comins, M.P. Hassell and R.M. May, J. Animal Ecology 61 (1992) 735.
[12] Y. Iwasa, K. Sato and S. Nakashima, J. Theoret. Biol. 152 (1991) 143.
[13] K. Sato and Y. Iwasa, Ecology 74 (1993) 1538.
[14] N. Kopell and L.N. Howard, Stud. Appl. Math. 52 (1973) 291.
[15] G.B. Ermentrout, Lecture Notes in Pure and Appl. Math. 54 (1980) 217.
[16] B. Schönfisch, Physica D 80 (1995) 433.
[17] M. Markus, Biomedi. Biochimi. Acta 49 (1990) 681.
[18] H.E. Schepers and M. Markus, Physica A 188 (1992) 337.
[19] T. Kkarapiperis and B. Blankleider, Physica D 78 (1994) 30.

[20] A.M. Turing, Philos. Trans. Roy. Soc. 237 (1952) 37.
[21] J.D. Murray, J. Theoret. Biol. 88 (1981) 161.
[22] J.R. Weimar, J.J. Tyson and L.T. Watson, Physica D 55 (1992) 309.
[23] J.R. Weimar, J.J. Tyson and L.T. Watson, Physica D 55 (1992) 328.
[24] M. Gerhardt, H. Schuster and J.J. Tyson, Physica D 46 (1990) 392.
[25] P.S. Hagan, SIAM J. Appl. Math. 42 (1982) 762.
[26] A.T. Winfree and S.H. Strogatz, Physica D 13 (1984) 221.
[27] Y. Kuramoto, Progr. Theoret. Phys. S 64 (1978) 346.
[28] A.B. Rovinsky, J. Phys. Chem. 91 (1987) 5113.
[29] J.A. Sherratt, Physica D 82 (1995) 165.
[30] K.R. Schneider, Zeitschrift Ang. Math. Phys. 34 (1983) 236.
[31] H.G. Othmer, Lectures Math. Life Sci. 9 (1977) 57.
[32] D. Cope, SIAM J. Appl. Math. 38 (1980) 457.
[33] K. Maginu, J. Differential Equations 31 (1979) 130.
[34] K. Maginu, J. Differential Equations. 39 (1981) 73.
[35] J.M. Greenberg, SIAM J. Appl. Math. 39 (1980) 301.
[36] S. Koga, Progr. Theoret. Phys. 67 (1982) 164.
[37] J.A. Sherratt, IMA J. Appl. Math. 52 (1994) 79.
[38] J.D. Murray, Mathematical Biology (Springer, Berlin, 1989).
[39] J.A. Sherratt, Physica D 70 (1994) 370.
[40] J.A. Sherratt, Int. J. Bifurc. Chaos 3 (1993) 1269.
[41] J.A. Sherratt, M.A. Lewis and A.C. Fowler, PNAS USA 92 (1995) 2524.
[42] J.A. Sherratt, SIAM J. Appl. Math. 54 (1994) 1374.
[43] J.A. Sherratt, Nonlinearity 6 (1993) 1055.
[44] M.W. Sabelis, O. Diekmann and V.A.A. Jansen, Biol. J. Linnean Soc. 42 (1991) 267.
[45] S.-N. Chow and W. Shen, Dynamics Systems and Applications 4 (1995) 1.